Generating ground motions using the Fourier amplitude spectrum

GENERATING GROUND MOTIONS USING THE FOURIER AMPLITUDE SPECTRUM

Marco Baglio[1], Alessandro Cardoni[1], Gian Paolo Cimellaro[1], Norman Abrahamson[2]

[1]Department of Structural, Geotechnical & Building Engineering, Politecnico di Torino, Corso Duca degli Abruzzi, 24, Turin, 10129, Italy.

[2]Department of Civil and Environmental Engineering, University of California Berkeley, California, 760 Davis Hall, CA 94720, United States.

In this paper a simplified method aimed at generating ground motions records using a Fourier amplitude spectrum model obtained by a response spectrum is presented. The use of white noise with specific conditions on the variance and inter-frequency correlation allows to get a realistic variability of the Fourier amplitude spectrum. Moreover, a two-corner frequency model is defined from empirical ground-motion data and a filter is applied to capture the attenuation at high frequencies. The generated series of stochastic ground motions accurately match the mean value of the target response spectrum. The procedure was tested on an Italian site and results showed excellent matching in terms of mean and dispersion values with either the median obtained from ground motion prediction equations and conditional mean spectra. The advantage of the proposed methodology is that time-histories can be generated with low computational effort, they do not need scaling or frequency content adjustments and are spectrum compatible with a given target spectrum.

KEYWORDS

Stochastic ground motion generation, phase derivatives, Fourier amplitude spectrum, target response spectrum, logistic distribution

INTRODUCTION

Real ground motion records are commonly used as input in structural dynamic analyses. The access to seismic record databases worldwide has been increasingly facilitated over the past few decades. The quality and size of those databases have also been constantly increasing. However, despite the efforts to extend the network of earthquake sensors, there are still some areas of the world where the earthquake records might not be enough to implement stochastic analyses. For instance, the Chilean fault system generates extremely strong and long ground motions that are not sufficiently represented in current databases. Moreover, there is still a lack of near-source records from large events making it difficult to establish whether observations are well representative of possible motions. In such cases it might be necessary to follow alternative methods that allow to generate synthetic ground motion records. Douglas and Aochi (2008)[1] presented a review of several methodologies that can be used to predict earthquake ground motions both in terms of time-histories and ground-motion intensity measures. In this research the focus is on methods that can be used to transform event parameters to acceleration time-histories. Generally, it is possible to categorize all methodologies in two approaches: physics-based and experimental-based. The first approach consists of mathematical models based on physical principles, while the second one relies on empirical data collected from previous seismic events fitted using various techniques. The models resulting from the second approach are not necessarily based on physical principles. Examples of physic-based approaches are Finite Element Methods (FEMs) and Spectral Element Methods (SEMs). FEMs and SEMs can be effectively used to model full 3D earthquake wave propagation even for strong motions[2], also considering variations of seismic wave velocity, density, and crustal thickness[3]. Nevertheless, they require high-resolution input data and considerable computational effort. On the other hand, experimental-based methods can be used to generate ground motion by filtering a random signal's frequency content and multiplying it by an envelope function. The frequency content and envelope function are usually defined through prediction equations such as those introduced by Sabetta and Pugliese (1996)[4] and Rathje et al. (1998)[5]. Some of these methodologies have been implemented in free and user-friendly software such as SIMQKE[6] and OPENSIGNAL[7] that embed several features to select ground motion records and do basic signal processing operations.

The lack of physicals principles of the experimental-based methods has shifted the focus of researchers on the first category, which offers the possibility to find solutions to a larger number of case studies. Boore (2003)[8] proposed one of the most exhaustive and simple stochastic methods based on the physics of the earthquake process and wave propagation. A Fourier Amplitude Spectrum (FAS) model is estimated using a point-source spectrum model, which

is transferred to the analyzed site by means of anelastic and geometric attenuation. The obtained FAS is used to filter a Gaussian white noise by following the same procedure used by the experimental approach. The natural evolution of this method is the discretization of the complex geometry of a given fault by combining several points-source spectra. Atkinson and Assatourians (2014)[9] described the implementation and validation of such methodology. In addition, a relationship between the response spectrum and the Fourier Amplitude Spectrum (FAS) was proposed by Gasparini and Vanmarcke (1976)[10]. In their research, random vibration theory is used to define the power spectral density function from a response spectrum through an iterative process. The FAS is obtained by energy equilibrium using the power spectral density function. Then, time histories are computed by superposition of sine waves shaped through an envelope function to accomplish non-stationarity. FAS models from this method are often inconsistent in low and high frequency ranges and require scaling to match the response spectrum. Thus, a process of adjustment in the frequency domain is necessary to improve the spectral matching.

In this paper, a new method to define a FAS model based on physics assumptions is proposed and used to generate spectrum compatible stochastic ground motions with respect to a given target spectrum. The approach is an extension of the stochastic simulation method proposed by Boore (2003)[8]. Compared to the original method, the first novelty of the proposed approach consists in adjusting the FAS model so that the simulated mean spectrum closely matches a target response spectrum. The second novelty concerns the introduction of phase derivatives. Typically, a white noise is windowed by an envelope function in the time domain and then filtered in the frequency domain. The effect of such windowing is a variation of the phase derivatives distribution (i.e., the derivative of phase angles) in the frequency domain. Their importance in signal non-stationarity was pointed out for the first time by Ohsaki (1979)[11]. The proposed phase derivatives distribution, consistent with magnitude, rupture distance and shear-wave velocity, allows to achieve time non-stationarity. Stochastic ground motions generated through this procedure show mean value and dispersion consistent with a target spectrum and an inter-frequency correlation consistent with the seismic records.

The proposed approach is intended to be used to generate time histories for use in nonlinear structural analyses when actual seismic records are missing or not enough to represent possible ground motions. It is also intended to be used along with the current seismic codes. Therefore, the method includes considerations relying on the elastic response spectrum. As several researchers pointed out the elastic response spectrum in association with the peak ground acceleration (PGA) might not be the most effective analysis tool to quantify inelastic deformations.[12,13] Nonlinear methods and probabilistic approaches to determine design seismic demands might be a better analysis tool and in some cases have shown better performances[14,15], especially in the case of pulse-like ground motions[16] and rupture directivity effects[17] which are potentially more damaging. The outcome of this research is however envisioned as a practical tool that can be effectively used by professional engineers, who comply with current design codes.

PROPOSED METHODOLOGY BASED ON A FOURIER AMPLITUDE SPECTRUM MODEL

The work-flow is based on the methodology presented by Boore (2003)[8], where the frequency content of a white noise is filtered by means of a FAS model and inverted in the time domain. The first step of the proposed methodology is based on the generation of a FAS model from a target response spectrum. The additive double corner frequency model proposed by Boore et al. (2014)[18] was adopted. Considering a flat high-frequency acceleration spectrum and equating the double corner frequencies (f_a; f_b) model to a single corner frequency (f_c) model, f_b can be related to f_a and f_c through Equation (1):

$$f_b = f_a \sqrt{\frac{(f_c / f_a)^2 - (1-\varepsilon)}{\varepsilon}} \tag{1}$$

where ε is a weighting parameter. Therefore, it is possible to write the double corner FAS model proposed by as shown in Equation (2):

$$A(f) = C\left[\frac{f^2(1-\varepsilon)}{1+\left(\frac{f}{f_a}\right)^2} + \frac{f^2\varepsilon}{1+\frac{f^2}{(f_c^2 - f_a^2)/\varepsilon + f_a^2}}\right] \quad (2)$$

where C is a scaling parameter. This is the generalized FAS model used to create the frequency amplitudes. To better represent the Fourier amplitudes at high frequencies, the model can be modified by applying a filter. In this study, the attenuation at high frequencies is modeled by applying the k filter[19] as described in Equation (3).

$$D(f) = e^{-\pi\kappa f} \quad (3)$$

The parameters ε, f_a and C should be thoroughly calibrated to match the low frequency part of the target response spectrum, while a proper value of k should be selected to fit the high frequency part. A novel procedure to determine the abovementioned variables was developed. It consists of the following steps:

1. A target spectrum associated to a specific value of moment magnitude (M) is computed either from ground motion prediction equations or using the conditional mean spectrum.
2. Twenty white noise samples are generated. No time windowing is applied. The duration of the signal should be properly set as it affects the spectrum.[20-22] To demonstrate the procedure a 10 s white noise is analyzed as this duration can be considered a lower limit to provide enough frequency resolution (Figure 1a). For each signal, the Fast Fourier Transform is computed, and the amplitude normalized by its root mean square (Figure 1b). The FAS of each sample is multiplied by the ω-square model according to Aki (1967)[23] as described in Equation (4).

$$\alpha(f) = \frac{2\pi f^2}{1+\left(\frac{f}{f_c}\right)^2} \quad (4)$$

The corner frequency value (f_c) is set based on the moment magnitude M associated to the target spectrum, and it is computed as $\log(f_c) = 2.623 - 0.5M$.[24] Amplitudes are then normalized by root mean square (Figure 1c). Finally, the time history can be obtained through the inverse Fourier Transform (Figure 1d).

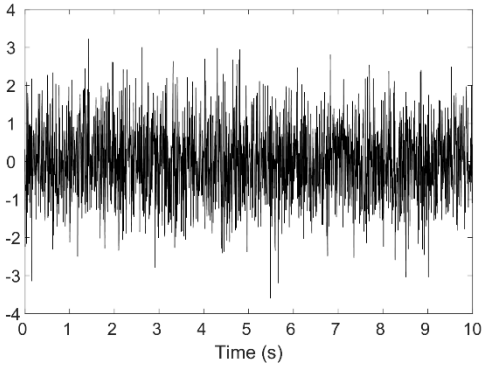

(a)

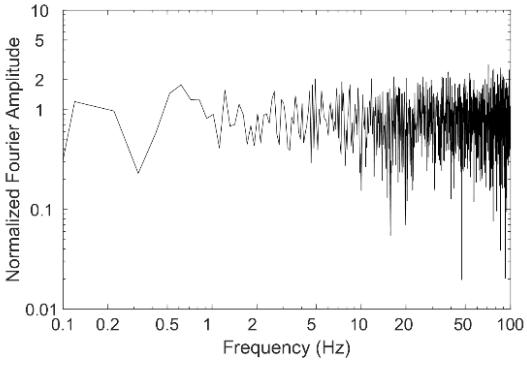

(b)

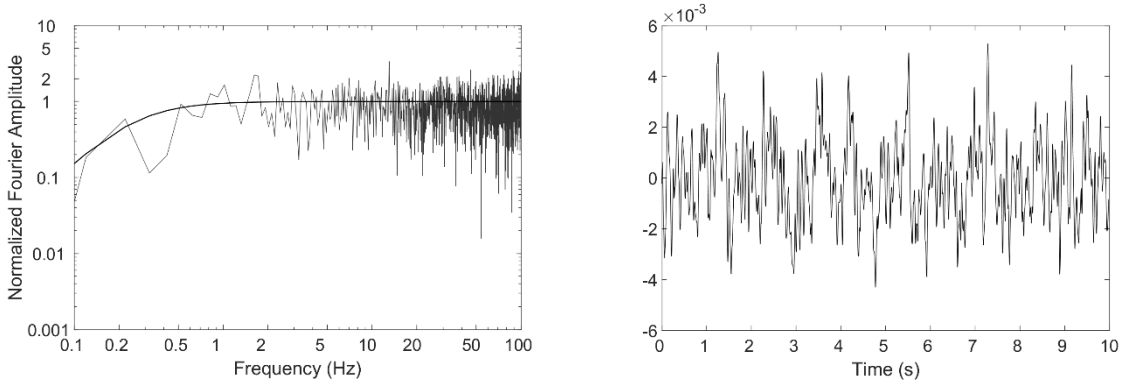

(c) (d)

Figure 1 - Description of the white noise generation and scaling process: (a) white noise generation; (b) Fourier amplitude spectrum computation and normalization by its root mean square; (c) Fourier amplitude spectrum scaled by the ω-square model; (d) time history obtained through inverse Fourier transform.

3. To ensure that the FAS matches the target spectrum, iterative adjustments are performed until reaching an acceptable mismatch. The iterative adjustments consist in multiplying the current Fourier amplitude (FA_i) by the ratio between the spectral acceleration of the target spectrum (Sa_T) and the spectral acceleration of the current FAS (Sa_i) (Figure 2a). The following formula (Equation (5)) describes the adjustment procedure.

$$FA_{i+1} = FA_i \frac{Sa_T}{Sa_i} \tag{5}$$

4. Non-linear regressions are used to estimate ε, f_a, and C (Figure 2b) needed for the FAS model (Equation (1)). The *least mean square* algorithm was used to perform nonlinear curve fitting. The algorithm estimates the best values for ε, f_a, and C that fits the nonlinear FAS model to the data obtained in the previous step.

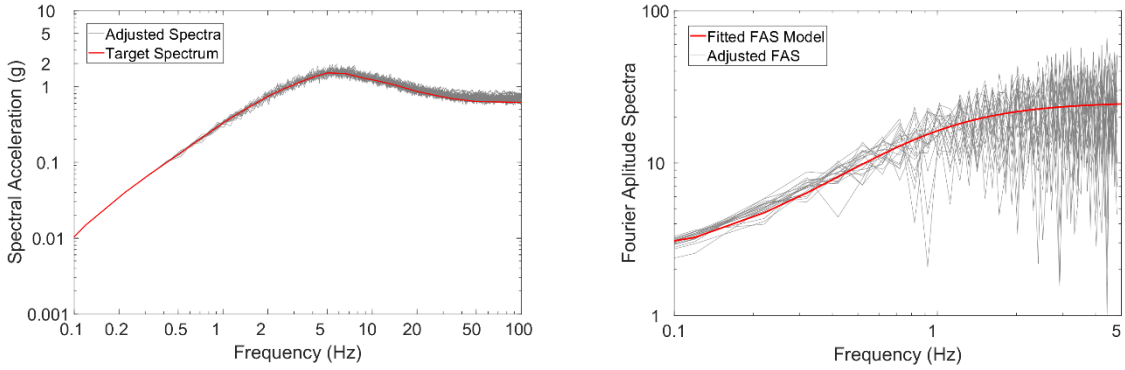

(a) (b)

Figure 2 - (a) Adjusted response spectra and (b) Fourier amplitude spectra of the adjusted samples.

5. Observations are generated by the calibrated FAS model defined in previous steps. The k filter in Equation (3) is then applied to the observation. A tentative value of k should be selected here. Following the recommendations of Boore and Joyner (1997)[25], a k value of 0.04 should be adequate as a first guess for a generic rock site. The procedure to generate different observations can be summarized as follow:
    a. Random Fourier amplitudes ($ln\ A(f)$) are computed using Equation (6) according to a multivariate normal distribution[26] characterized by a mean vector $FA(\varepsilon, f_a, C, f_c, f)$, where FA is the fitted FAS model, and a covariance matrix $\boldsymbol{\Sigma}(f)$:

$$\ln A(f) \sim N[FA(C, f_a, \varepsilon, f_c, f), \sum(f)] \quad (1)$$

b. Random phase angles are computed according to a uniform distribution. At this stage it is not necessary to have time non-stationarity, thus generating random phase angles uniformly distributed is computationally more efficient.
c. The inverse Fourier transform is computed to obtain the simulated accelerograms.

6. A response spectrum for each realization is defined and the mean response spectrum is computed.
7. The mean response spectrum and the target spectrum are compared to verify if they match in the short period range. If the level of matching is not satisfactory, the procedure goes back to step 5 where another *k* filter should be selected. The iteration continues until the desired error tolerance is achieved.
8. Time-histories are obtained from the FAS model using the estimated ε, f_a, C and k value from the previous steps. The procedure is similar to the one described in step 5, although in this case random *logistic-distributed* phase angles (x) are computed to accomplish time non-stationarity. Logistic distribution is a normal distribution with higher kurtosis defined by a mean (μ) and a scale parameter (σ). The proposed logistic distribution has been selected since the phase derivative distributions were observed to be fat-tailed. The logistic probability density function is described by (Equation (7)).

$$f(x;\mu,\sigma) = \frac{e^{-\frac{x-\mu}{\sigma}}}{\sigma\left(1+e^{-\frac{x-\mu}{\sigma}}\right)^2} \quad (7)$$

The value of the mean (μ) of the distribution is not relevant in this case and thus can be chosen arbitrarily. For simplicity, μ was set equal to π/df in order to have a distribution cantered around the peak. Then by simply multiplying by df it is possible to obtain the phase differences that are used to generate the phase angles. On the other hand, the scale parameter (σ) must be defined. In this work, the scale parameter was related to the effective duration (*SD*), which has the advantages of considering the characteristics of the entire accelerogram and defining a time frame where the ground motion is strong.[27] The proposed relationship between σ and *SD* is shown in Equation (8).

$$log(\sigma / \pi) = \alpha_1 + \alpha_2 log(SD) \quad (8)$$

Different models can be used to define SD. In this work SD is considered as the sum of duration contributions dependent on magnitude (D_M), rupture distance (D_{Rrup}) and shear-wave velocity (D_{Vs30}):

$$SD = D_M + D_{R_{rup}} + D_{V_{s30}} \quad (9)$$

The seismic source model of Boore (2003)[8] describes the influence of magnitude on duration through the expression $D_M = 1/f_c$. Atkinson and Boore (1995)[28] proposed a linear relation between the duration and the rupture distance: $D_{R_{rup}} = \beta_3 R_{Rup}$. The dependence of duration on the near-surface shear-wave velocity is accounted through the following relation: $D_{Vs30} = \beta_4 \log(V_{S30})$.

Consequently, the relationship used to estimate the scale parameter σ becomes (Equation (10)):

$$log(\sigma / \pi) = \alpha_1 + \alpha_2 log[\beta_1 + \beta_2 / f_c + \beta_3 R_{rup} + \beta_4 \log(V_{s30})] \quad (10)$$

Therefore, two steps of regression are needed. The first one is a linear regression to determine the coefficients α_1 and α_2 while the second one is a non-linear regression to define β_1, β_2, β_3, and β_4.

CASE STUDY AND DISCUSSION OF THE RESULTS

The fitted FAS model was tested using four target spectra. The first one is derived from the ground motion prediction equation (GMPE) presented by Abrahamson et al. (2014)[29] which is based on the NGA-West2 database.[30] Table 1 reports the parameters that were used to calculate the geometric mean.[31-34]

Table 1 - Weight coefficients used for the computation of the NGA-West2 GMPE geometric mean.

ASK	BSSA	CB	CY	IM
0.22	0.22	0.22	0.22	0.12

The other parameters for the computation of the GMPE are related to the town of Francofonte (Sicily, Italy) and are shown in Table 2.

Table 2 - Parameters used in GMPE computation. Omitted values are set as unknown.

M	R_{rup} [km]	R_{jb} [km]	R_x [km]	R_{y0} [km]	V_{s30} [m/s]	F_{rv}	F_{nm}	F_{hw}	Dip [°]	Z_{tor} [km]
7	6	4.47	-4.47	-	760	1	-	-	45	4

The GMPE was then used to compute the other three conditional mean spectra (CMS) starting from a uniform hazard spectrum (UHS) conditioned on a 2475-year return period, according to the Italian seismic hazard map. The selected structural periods for the three CMS were 0.2s, 0.5s, and 1.0s, respectively (Figure 3a). Each target spectrum was obtained as follows:

1. Calculate FAS model parameters and the *k-filter* using the procedure described in previous section. The duration of the generated signals was set to 15 s, which is about the effective duration (*SD*) obtained from the site and event parameters.
2. Generate a set of 1,000 stochastic ground motions using random logistic-distributed phase angles to obtain non-stationarity.
3. Apply a baseline correction and a Butterworth low-frequency filter with a cut-off frequency of 0.02 Hz.
4. Exclusively for CMS, remove each time-history that exceeds the mean of the target standard deviation (σ) of 2.5 times. Moreover, the logarithmic standard deviation is lower bounded at 0.15 to avoid pinching phenomena in the conditioning period.

Applying the step-by-step procedure to the Francofonte case study, it is possible to verify that the FAS models are consistent with the target spectra (Figure 3b). In particular, the 1.0 s CMS highlights the model's flexibility, as demonstrated by higher Fourier amplitudes at low frequencies.

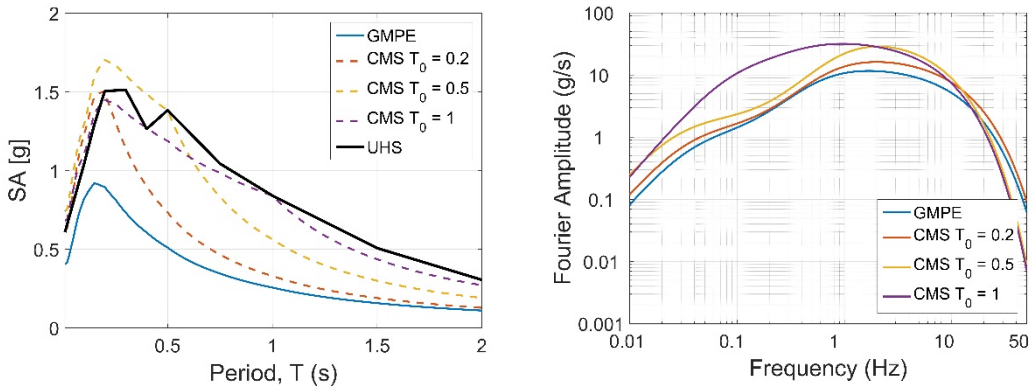

(a) (b)

Figure 3 - (a) GMPE, CMS, UHS and (b) the fitted FAS model for the Francofonte case study.

It is worth noting that FAS model parameters' computation includes a multivariable analysis. For each target spectrum, Figure 4 illustrates the region of possible f_a-ε pairs for a fixed C, shaded based on the coefficient of determination (R^2). As long as this case study is concerned, best pairs in terms of R^2 happen to be for ε values around 0.1, and they are far from the f_{lim}, i.e. the f_a upper bound, calculated as expressed in Equation (11).

$$f_{\lim} = \sqrt{\frac{1}{1-\varepsilon}} f_c \tag{11}$$

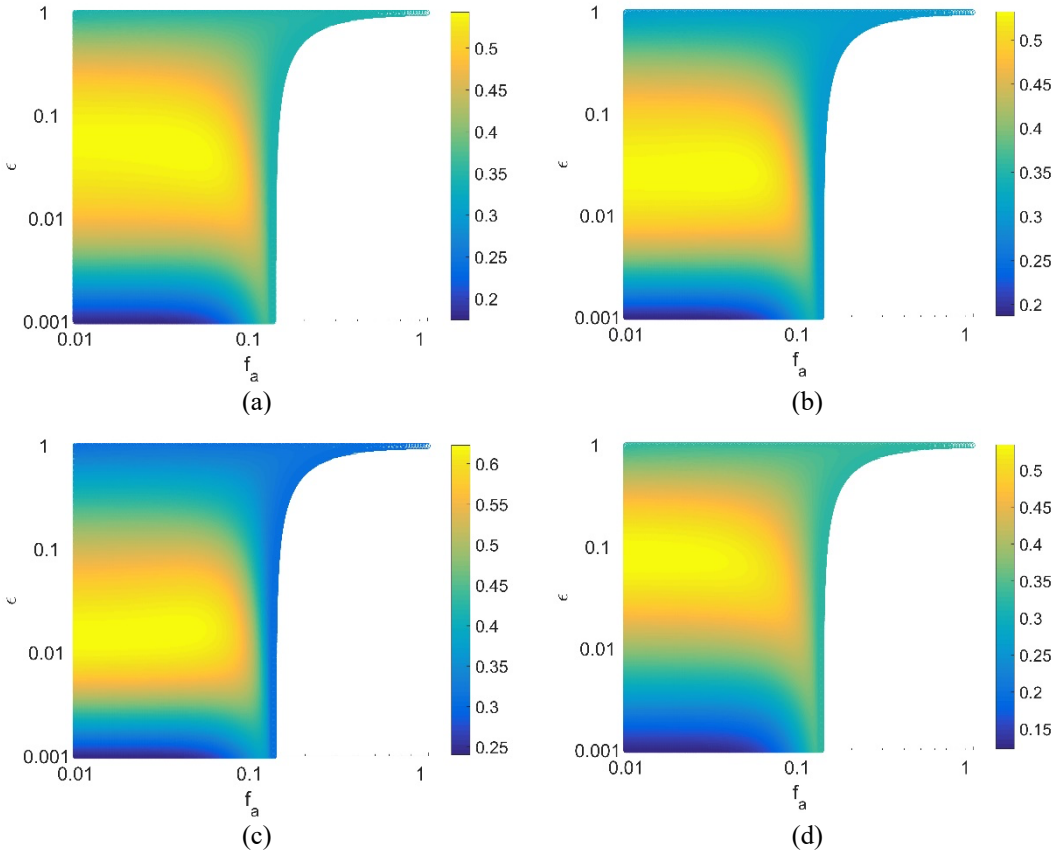

Figure 4 - f_a - ε solution pairs for (a) GMPE, (b) 0.2 s CMS, (c) 0.5 s CMS, (d) 1.0 s CMS.

Figure 5 shows the series of simulated spectra and their mean for each of the four target spectra. As it can be seen, the simulated mean spectrum (continuous red curve) precisely matches the target (dashed blue curve). The effect of duration in the generation of the FAS model was also investigated. The analysis was repeated considering signal durations of 10 s, 20 s, 30 s, 40 s for each of the CMS. As it can be seen from Figure 6, the duration has a limited effect on the results as the simulated spectra are all closely matching the target spectrum. The correlation coefficients (ρ) between each simulated mean spectrum and the target were also computed. The results obtained for the 10s duration seems still acceptable with a correlation coefficient of about 0.93 in the worst case (i.e., 0.2 s CMS). Increasing the duration, it is possible to notice a slight improvement of 2% in the correlation coefficients, reaching an almost perfect correlation between the simulated and the target spectrum.

A more evident demonstration of this outcome is presented in Figure 7, where the logarithmic residuals are analyzed. The continuous black line is the mean bias, whereas the light gray shading depicts the standard deviation, and the dark shading represents a 90% confidence region on the mean bias. Logarithmic residuals vary within a range of about ±0.2, which can be considered a solid matching.

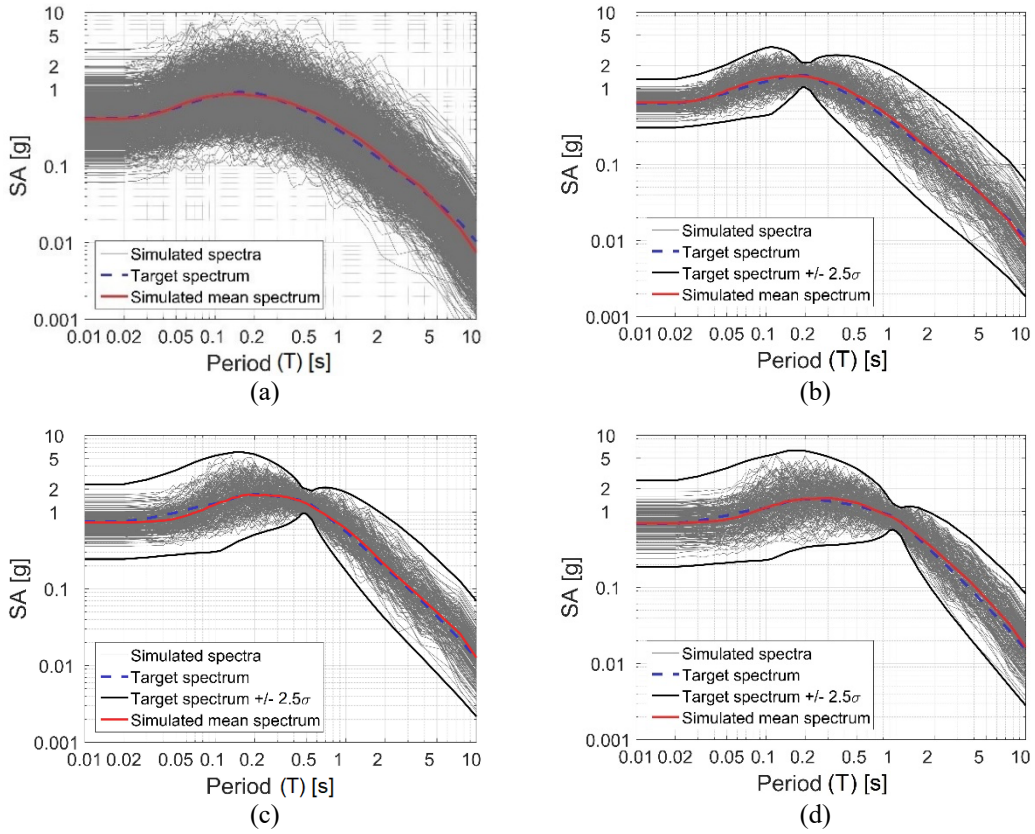

Figure 5 - Simulated spectra for (a) GMPE, (b) 0.2s CMS, (c) 0.5s CMS, (d) 1.0s CMS.

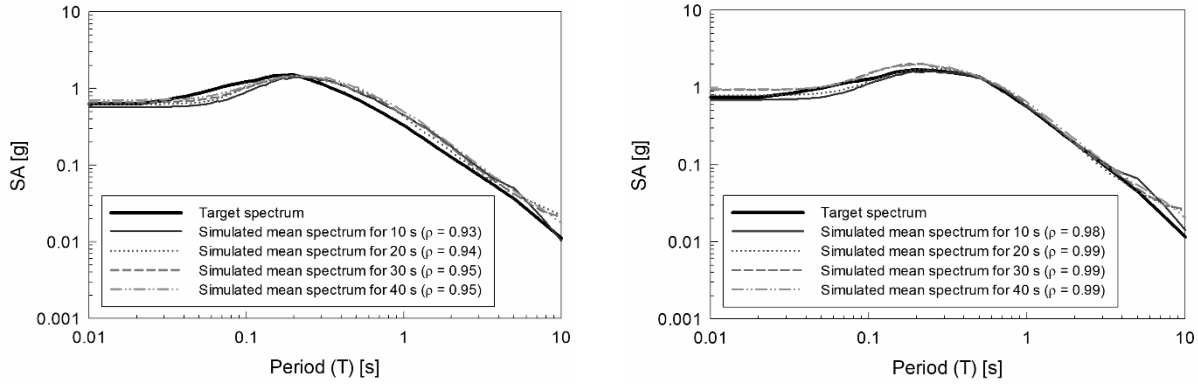

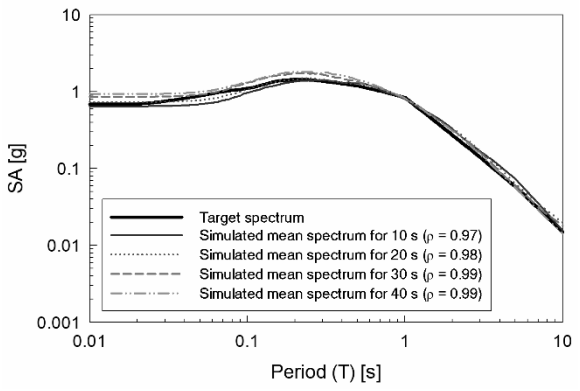

(c)

Figure 6 - Comparison of simulated mean spectra obtained for different durations for (a) 0.2s CMS, (b) 0.5s CMS, and (c) 1.0s CMS.

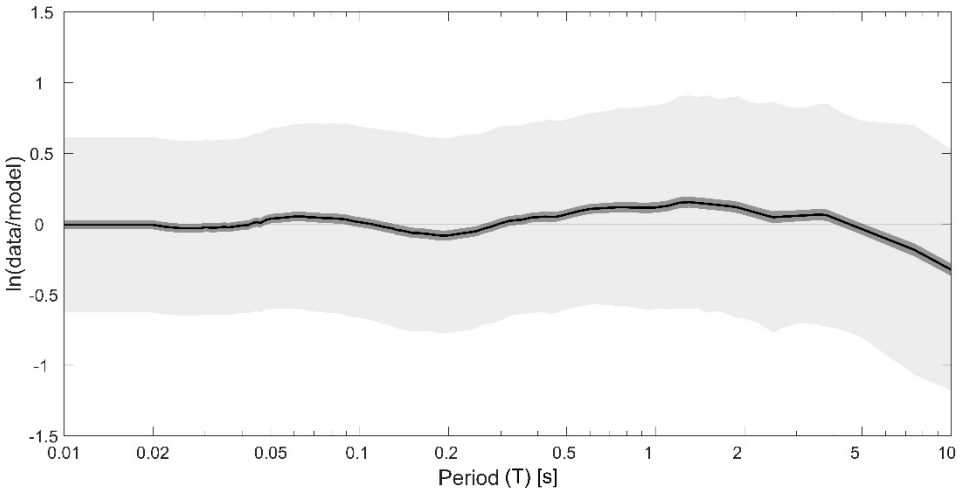

(a)

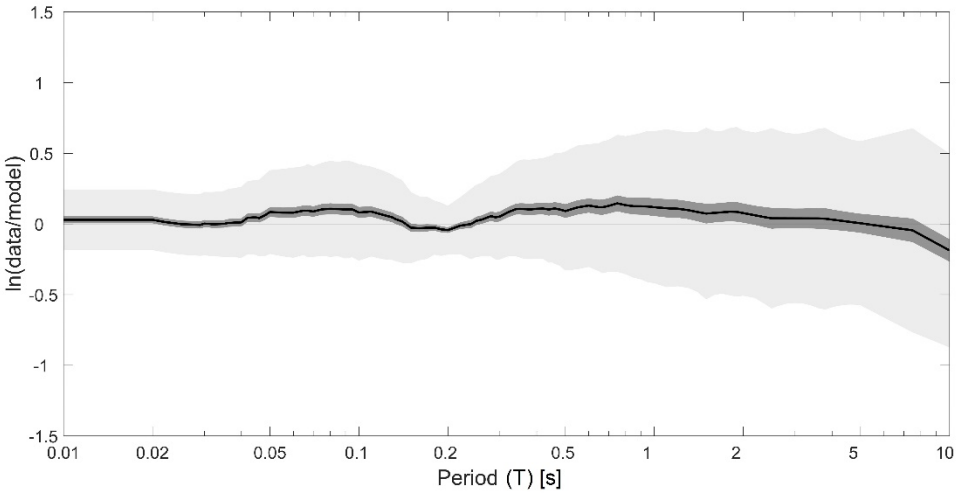

(b)

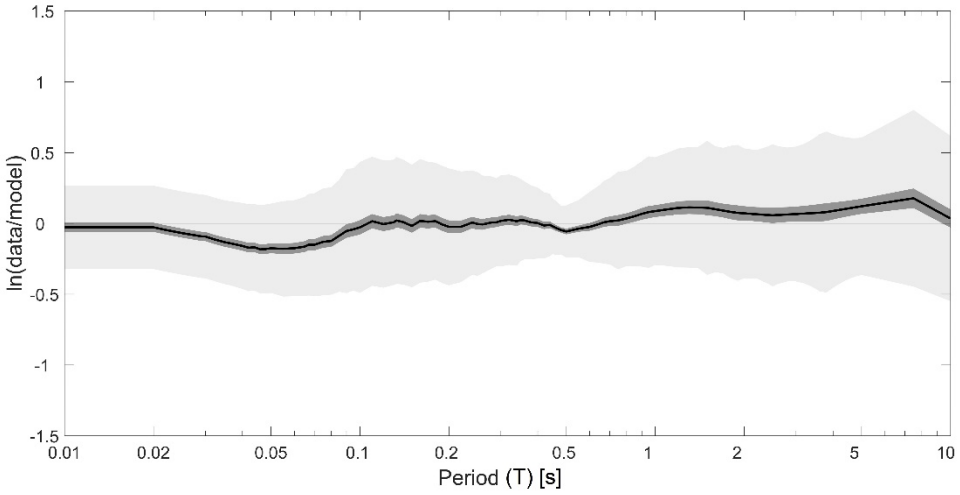

(c)

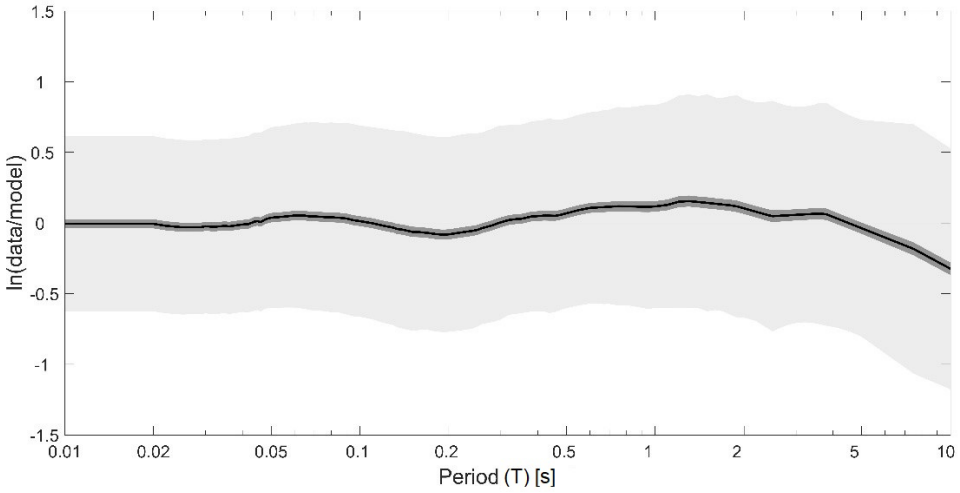

(d)

Figure 7 - Accuracy of fitted models in terms of logarithmic residuals for (a) GMPE, (b) 0.2s CMS, (c) 0.5s CMS, (d) 1.0s CMS.

In addition, a measure of dispersion is provided comparing the logarithmic standard deviation between the target spectrum and simulated spectra. The variance in the input FAS model was assumed to be constant and equal to 0.8. This assumption allows to generate a dispersion consistent with the GMPE's standard deviation as shown in Figure 8.

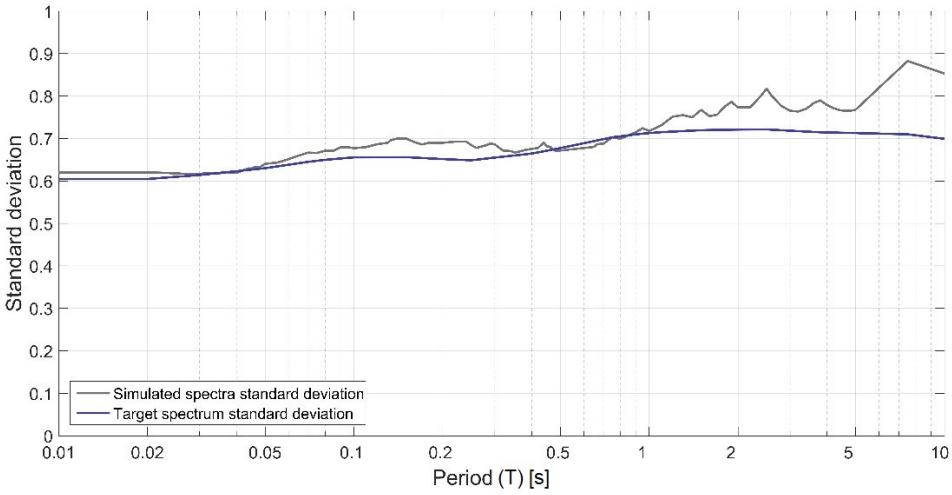
Standard deviation
Period (T) [s]
Simulated spectra standard deviation
Target spectrum standard deviation

(a)

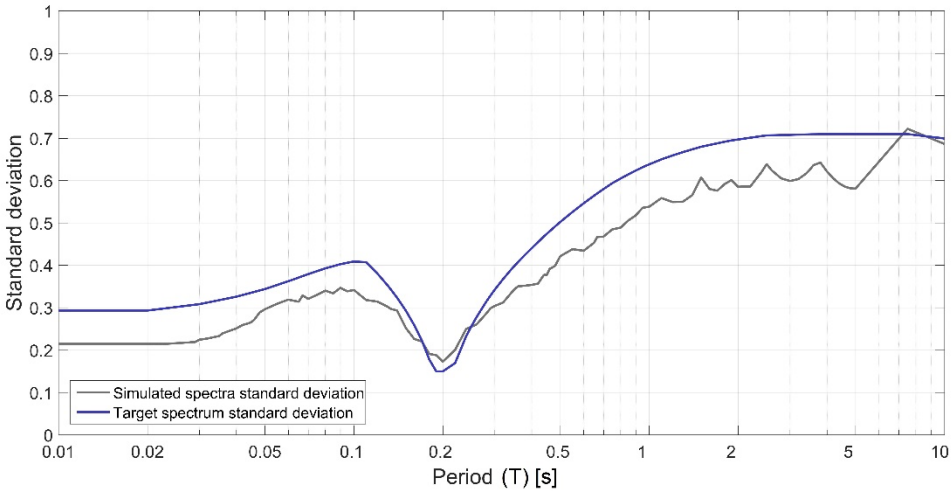
Standard deviation
Period (T) [s]
Simulated spectra standard deviation
Target spectrum standard deviation

(b)

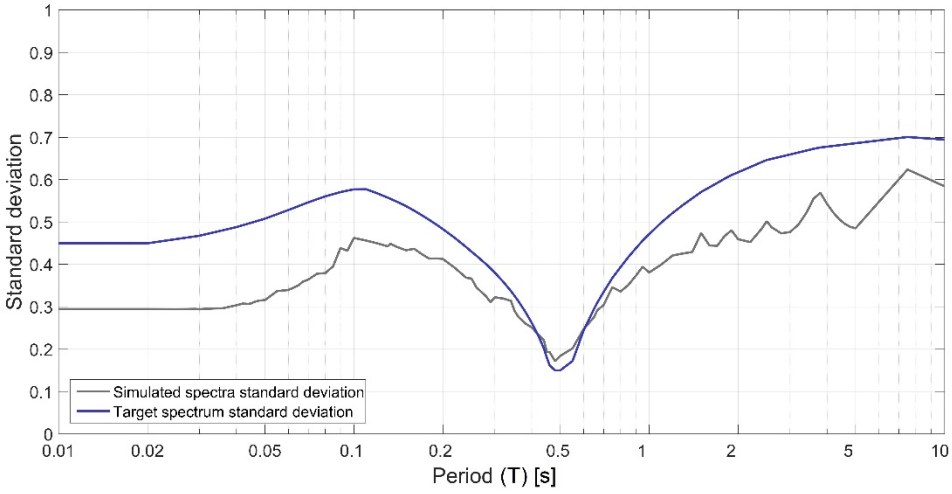
Standard deviation
Period (T) [s]
Simulated spectra standard deviation
Target spectrum standard deviation

(c)

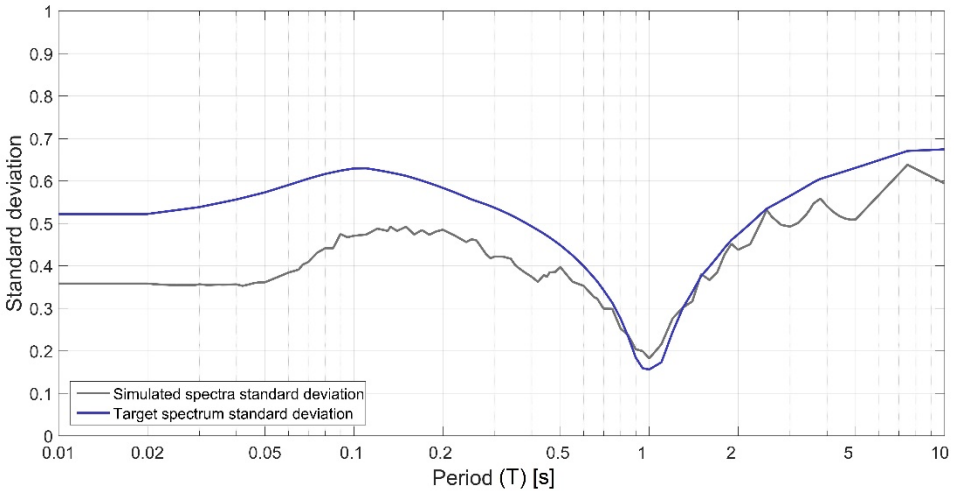

(d)

Figure 8 - Logarithmic standard deviation comparison between (a) GMPE, (b) 0.2s CMS, (c) 0.5s CMS, (d) 1.0s CMS.

However, the comparison with CMS standard deviation pointed out an overall underestimation of the dispersion when far from the corresponding conditioning period. This behavior is determined by the inter-frequency correlation model implemented for the FAS generation. The model proposed by Stafford (2017)[26] was used in the generation of stochastic ground motions. The two main terms of Equation (6) are the mean vector $FA(C, f_a, \varepsilon, f_c, f)$, and the covariance matrix $\boldsymbol{\Sigma}(f)$, which can be expressed as shown by Equation (12):

$$\sum(f) = \begin{bmatrix} \sigma^2(f_1) & \rho(f_1,f_2)\sigma(f_1)\sigma(f_2) & \cdots & \rho(f_1,f_n)\sigma(f_1)\sigma(f_n) \\ \rho(f_2,f_1)\sigma(f_2)\sigma(f_1) & \sigma^2(f_2) & \cdots & \rho(f_2,f_n)\sigma(f_2)\sigma(f_n) \\ \vdots & \vdots & \ddots & \vdots \\ \rho(f_n,f_1)\sigma(f_n)\sigma(f_1) & \rho(f_n,f_2)\sigma(f_1)\sigma(f_2) & \cdots & \sigma^2(f_n) \end{bmatrix} \quad (12)$$

where $\sigma(f_i)$ is the standard deviation relative to the frequency f_i, and $\rho(f_i, f_j)$ is the correlation between f_i and f_j frequencies. They depend on three different contributions: between-event component (E), within-event component (A) and between-site component (S). They are explicitly calculated as indicated in Equation (13) and Equation (14).

$$\rho(f_i,f_j) = \frac{\rho_E(f_i,f_j)\sigma_E(f_i)\sigma_E(f_j) + \rho_A(f_i,f_j)\sigma_A(f_i)\sigma_A(f_j) + \rho_S(f_i,f_j)\sigma_S(f_i)\sigma_S(f_j)}{\sigma(f_i)\sigma(f_j)} \quad (13)$$

$$\sigma^2(f_i) = \sigma_E^2(f_i) + \sigma_A^2(f_i) + \sigma_S^2(f_i) \quad (14)$$

A test was carried out on the 1,000 simulated spectra from GMPE to check the consistency of the obtained correlation and the inter-frequency correlation model.

Figure 9a shows the correlation computed from logarithmic residuals of FAS model. Comparing this result to the adopted model, it is possible to confirm the inter-frequency correlation in the FAS model (Figure 9b).

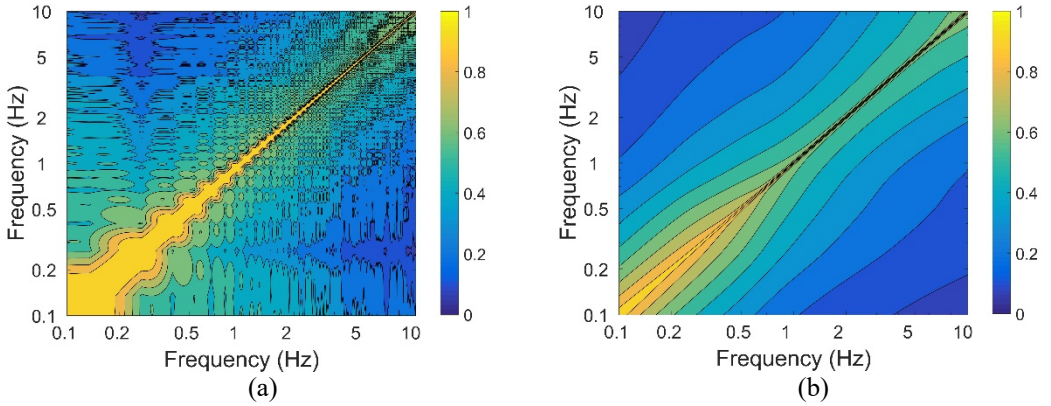

Figure 9 - Correlation analysis of the FAS logarithmic residuals for: (a) the series of stochastic ground motions and (b) the model proposed by Stafford (2017)[26].

A further correlation test was performed on the spectral acceleration based on the model proposed by Baker and Jayaram (2008)[35]. A correction in the high frequencies was applied according to Carlton and Abrahamson (2014)[36].

Figure 10 depicts the comparison between the correlation obtained from the series of the stochastic ground motions and the model. Overall, it shows consistency in the shape of the two shaded regions, although overestimation is detected, especially for low periods. Such difference is due to the underestimation of dispersion obtained from the CMS. Therefore, the standard deviation is more correlated to the conditioning period than to the adopted model.[35]

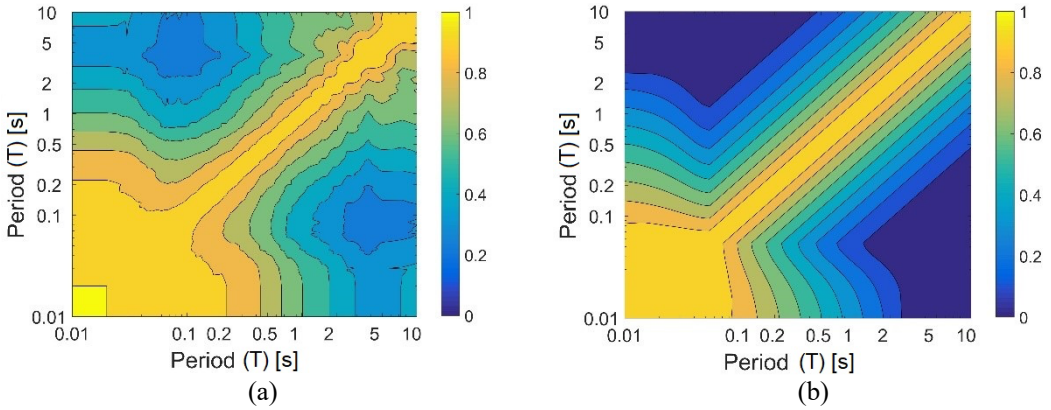

Figure 10 - Correlation analysis of the spectral acceleration for: (a) the series of stochastic ground motions and (b) the model proposed by Baker and Jayaram (2008)[35].

The proposed methodology can also be applied to obtain a series of stochastic ground motions compatible with a design spectrum. As an example, a design spectrum was calculated in accordance with the provisions of Eurocode 8[37] considering a ground acceleration (a_g) equal to 0.8g and a "C" soil category. The FAS model parameters were generated through the procedure described previously. In this case a set of 50 stochastic ground motions was computed, while the k filter was set to 0.08. Among these, only the simulated spectra within the range of target spectrum $\pm\sigma$ were considered.

Figure 11 shows 35 simulated spectra that were selected from the set of 50 realizations. The average spectrum (continuous red line) obtained from this set satisfies the spectrum compatibility required by Eurocode 8.[37]

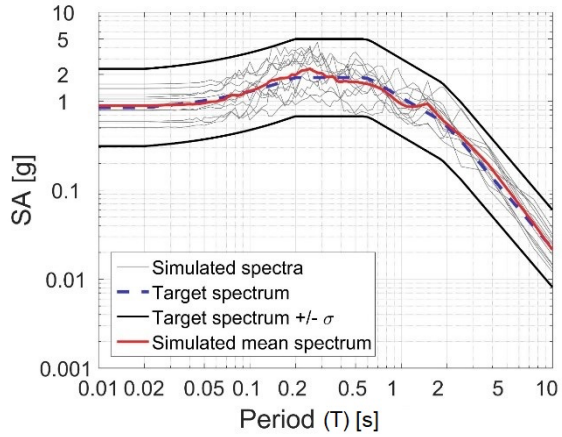

Figure 11 – Example of simulated spectra matching a design spectrum calculated according to Eurocode 8.

CONCLUSIONS

In this paper a method to obtain a Fourier amplitude spectrum model (FAS) from a response spectrum is presented. Non-linear regression is used to get a FAS model from a set of white-noise samples adjusted to match the response spectrum. The application of a k filter ensures the matching also in the low period region of the target response spectrum.

The implemented methodology allows the generation of a series of stochastic ground motions characterized by a mean value that matches a target response spectrum accurately. The time non-stationarity is achieved by including a phase derivatives distribution. It could be also possible to obtain non-stationarity in the frequency content by defining a function that describes the Fourier amplitude variation with time or by applying a phase derivative distribution dependent on the frequency content. Furthermore, the FAS is generated by means of a covariance matrix. This leads to three main advantages: (i) a dispersion consistent with the target spectrum obtained by adjusting the variance; (ii) an inter-frequency correlation consistent with the seismic records; (iii) low computational effort.

The procedure has been tested on series of simulated spectra generated from a ground motions prediction equation. Numerical results have shown solid matching in terms of mean and dispersion values. Further analyses demonstrated how this methodology can be successfully applied also with conditional mean spectra (CMS). In addition, an inter-frequency correlation model is introduced, which allows to generate an FAS with proper variability and correlation. Results are consistent with the model, despite a general overestimation is observed, especially in the low period range. This is potentially due to the underestimation of dispersion obtained from the CMS.

ACKNOWLEDGMENTS

The research leading to these results has received funding from the European Research Council under the Grant Agreement n°ERC_IDEal reSCUE_637842 of the project IDEAL RESCUE—Integrated DEsign and control of Sustainable CommUnities during Emergencies.

DATA AVAILABILITY STATEMENT

The data that support the findings of this study are available from the corresponding author upon reasonable request.

REFERENCES

1. Douglas J, Aochi H. A survey of techniques for predicting earthquake ground motions for engineering purposes. *Surveys in geophysics*. 2008;29(3):187.

2. Ichimura T, Hori M, Kuwamoto H. Earthquake motion simulation with multiscale finite-element analysis on hybrid grid. *Bulletin of the Seismological Society of America*. 2007;97(4):1133-1143.
3. Komatitsch D, Ritsema J, Tromp J. The spectral-element method, Beowulf computing, and global seismology. *Science*. 2002;298(5599):1737-1742.
4. Sabetta F, Pugliese A. Estimation of response spectra and simulation of nonstationary earthquake ground motions. *Bulletin of the Seismological Society of America*. 1996;86(2):337-352.
5. Rathje EM, Abrahamson NA, Bray JD. Simplified frequency content estimates of earthquake ground motions. *Journal of Geotechnical and Geoenvironmental Engineering*. 1998;124(2):150-159.
6. Gasparini D, Vanmarcke EH. SIMQKE: A program for artificial motion generation. *Department of Civil Engineering, Massachusetts Institute of Technology, Cambridge, MA*. 1976;
7. Cimellaro GP, Marasco S. A computer-based environment for processing and selection of seismic ground motion records: OPENSIGNAL. *Frontiers in Built Environment*. 2015;1:17.
8. Boore DM. Simulation of ground motion using the stochastic method. *Pure and applied geophysics*. 2003;160(3-4):635-676.
9. Atkinson GM, Assatourians K. Implementation and validation of EXSIM (a stochastic finite-fault ground-motion simulation algorithm) on the SCEC broadband platform. *Seismological Research Letters*. 2014;86(1):48-60.
10. Gasparini DA, Vanmarcke EH. *Simulated Earthquake Motions Compatible with Prescribed Response Spectra*. Massachusetts Institute of Technology, Department of Civil Engineering, Constructed Facilities Division; 1976.
11. Ohsaki Y. On the significance of phase content in earthquake ground motions. *Earthquake Engineering & Structural Dynamics*. 1979;7(5):427-439.
12. Bradley BA. A comparison of intensity-based demand distributions and the seismic demand hazard for seismic performance assessment. *Earthquake Engineering & Structural Dynamics*. 2013;42(15):2235-2253.
13. Haselton CB, Baker JW, Stewart JP, et al. Response history analysis for the design of new buildings in the NEHRP provisions and ASCE/SEI 7 standard: Part I-Overview and specification of ground motions. *Earthquake Spectra*. 2017;33(2):373-395.
14. Bradley BA. Design seismic demands from seismic response analyses: a probability-based approach. *Earthquake Spectra*. 2011;27(1):213-224.
15. Jayaram N, Lin T, Baker JW. A computationally efficient ground-motion selection algorithm for matching a target response spectrum mean and variance. *Earthquake spectra*. 2011;27(3):797-815.
16. Iervolino I, Chioccarelli E, Baltzopoulos G. Inelastic displacement ratio of near-source pulse-like ground motions. *Earthquake Engineering & Structural Dynamics*. 2012;41(15):2351-2357.
17. Baltzopoulos G, Luzi L, Iervolino I. Analysis of near-source ground motion from the 2019 Ridgecrest earthquake sequence. *Bulletin of the Seismological Society of America*. 2020;110(4):1495-1505.
18. Boore DM, Di Alessandro C, Abrahamson NA. A generalization of the double-corner-frequency source spectral model and its use in the SCEC BBP Validation Exercise. *Bulletin of the Seismological Society of America*. 2014;104(5):2387-2398.
19. Anderson JG, Hough SE. A model for the shape of the Fourier amplitude spectrum of acceleration at high frequencies. *Bulletin of the Seismological Society of America*. 1984;74(5):1969-1993.
20. Bora SS, Scherbaum F, Kuehn N, Stafford P. On the relationship between Fourier and response spectra: Implications for the adjustment of empirical ground-motion prediction equations (GMPEs). *Bulletin of the Seismological Society of America*. 2016;106(3):1235-1253.
21. Van Houtte C, Larkin T, Holden C. On Durations, Peak Factors, and Nonstationarity Corrections in Seismic Hazard Applications of Random Vibration TheoryOn Durations, Peak Factors, and Nonstationarity Corrections in Seismic Hazard Applications of RVT. *Bulletin of the Seismological Society of America*. 2018;108(1):418-436.
22. Kolli MK, Bora SS. On the use of duration in random vibration theory (RVT) based ground motion prediction: a comparative study. *Bulletin of Earthquake Engineering*. 2021;19:1687-1707.
23. Aki K. Scaling law of seismic spectrum. *Journal of Geophysical Research*. 1967;72(4):1217-1231.
24. Frankel AD, Mueller C, Barnhard T, et al. *National seismic-hazard maps: documentation June 1996*. US Geological Survey Reston, VA; 1996.
25. Boore DM, Joyner WB. Site amplifications for generic rock sites. *Bulletin of the seismological society of America*. 1997;87(2):327-341.
26. Stafford PJ. Interfrequency Correlations among Fourier Spectral Ordinates and Implications for Stochastic Ground-Motion Simulation. *Bulletin of the Seismological Society of America*. 2017;doi:10.1785/0120170081

27. Bommer JJ, Martínez-Pereira A. The effective duration of earthquake strong motion. *Journal of earthquake engineering*. 1999;3(02):127-172.
28. Atkinson GM, Boore DM. Ground-motion relations for eastern North America. *Bulletin of the Seismological Society of America*. 1995;85(1):17-30.
29. Abrahamson NA, Silva WJ, Kamai R. Summary of the ASK14 ground motion relation for active crustal regions. *Earthquake Spectra*. 2014;30(3):1025-1055.
30. Ancheta TD, Darragh RB, Stewart JP, et al. NGA-West2 database. *Earthquake Spectra*. 2014;30(3):989-1005.
31. Boore DM, Stewart JP, Seyhan E, Atkinson GM. NGA-West2 equations for predicting PGA, PGV, and 5% damped PSA for shallow crustal earthquakes. *Earthquake Spectra*. 2014;30(3):1057-1085.
32. Campbell KW, Bozorgnia Y. NGA-West2 ground motion model for the average horizontal components of PGA, PGV, and 5% damped linear acceleration response spectra. *Earthquake Spectra*. 2014;30(3):1087-1115.
33. Chiou BS-J, Youngs RR. Update of the Chiou and Youngs NGA model for the average horizontal component of peak ground motion and response spectra. *Earthquake Spectra*. 2014;30(3):1117-1153.
34. Idriss I. An NGA-West2 empirical model for estimating the horizontal spectral values generated by shallow crustal earthquakes. *Earthquake Spectra*. 2014;30(3):1155-1177.
35. Baker JW, Jayaram N. Correlation of spectral acceleration values from NGA ground motion models. *Earthquake Spectra*. 2008;24(1):299-317.
36. Carlton B, Abrahamson N. Issues and approaches for implementing conditional mean spectra in practice. *Bulletin of the Seismological Society of America*. 2014;104(1):503-512.
37. CEN. Eurocode 8: Design of structures for earthquake resistance, Part 1: General rules, seismic actions and rules for buildings. European Committee for Standardization Brussels; 2004.

LIST OF FIGURE CAPTIONS

Figure 1 - Description of the white noise generation and scaling process: (a) white noise generation; (b) Fourier amplitude spectrum computation and normalization by its root mean square; (c) Fourier amplitude spectrum scaled by the ω-square model; (d) time history obtained through inverse Fourier transform.

Figure 2 - (a) Adjusted response spectra and (b) Fourier amplitude spectra of the adjusted samples.

Figure 3 - (a) GMPE, CMS, UHS and (b) the fitted FAS model for the Francofonte case study.

Figure 4 - fa - ε solution pairs for (a) GMPE, (b) 0.2 s CMS, (c) 0.5 s CMS, (d) 1.0 s CMS.

Figure 5 - Simulated spectra for (a) GMPE, (b) 0.2s CMS, (c) 0.5s CMS, (d) 1.0s CMS.

Figure 6 - Comparison of simulated mean spectra obtained for different durations for (a) 0.2s CMS, (b) 0.5s CMS, and (c) 1.0s CMS.

Figure 7 - Accuracy of fitted models in terms of logarithmic residuals for (a) GMPE, (b) 0.2s CMS, (c) 0.5s CMS, (d) 1.0s CMS.

Figure 8 - Logarithmic standard deviation comparison between (a) GMPE, (b) 0.2s CMS, (c) 0.5s CMS, (d) 1.0s CMS.

Figure 9 - Correlation analysis of the FAS logarithmic residuals for: (a) the series of stochastic ground motions and (b) the model proposed by Stafford (2017)[26].

Figure 10 - Correlation analysis of the spectral acceleration for: (a) the series of stochastic ground motions and (b) the model proposed by Baker and Jayaram (2008)[35].

Figure 11 – Example of simulated spectra matching a design spectrum calculated according to Eurocode 8.